J. Environ. Syst. and Eng., JSCE, No. 692/VII-21, 83-97, 2001 November

SIMULATION OF THE PROBABILITY OF OCCURRENCE OF HYPOXIC AND ANOXIC WATER IN A COASTAL BAY DUE TO EUTROPHICATION AND LAND RECLAMATION

Md. Rezaul KARIM[1], Masahiko SEKINE[2], Takaya HIGUCHI[3] and Masao UKITA[4]

[1]Student Member of JSCE, M. Sc. Eng., Graduate Student, Dept. of Civil Eng., Yamaguchi University (2-16-1, Tokiwadai, Ube 755-8611, Japan)
[2]Member of JSCE, Dr. of Eng., Associate Professor, Dept. of Civil Eng., Yamaguchi University (2-16-1, Tokiwadai, Ube 755-8611, Japan)
[3]Member of JSCE, Dr. of Eng., Research Associate, Dept. of Civil Eng., Yamaguchi University (2-16-1, Tokiwadai, Ube 755-8611, Japan)
[4]Member of JSCE, Dr. of Eng., Professor, Dept. of Civil Eng., Yamaguchi University (2-16-1, Tokiwadai, Ube 755-8611, Japan)

In order to analyze the processes contributing to the formation of oxygen depleted waters and the subsequent probability of occurrence of hypoxia and anoxia in the inner Hakata Bay, a combined hydrodynamic and eutrophication model was developed. Comparison of yearlong calculation results with monitoring data shows that the model could represent reasonably the important features regulating water quality and dissolved oxygen of the bay. Hypoxia and anoxia are developed in the bottom waters in summer due to the presence of stratification caused by freshwater inflow and meteorological conditions and are most severe during August. The ongoing land reclamation work has insignificant impact on water quality, but it prolongs the duration of hypoxia and anoxia in the bay.

Key Words: probability of occurrence, anoxia and hypoxia, hydrodynamics, eutrophication, sediment-water interaction, land reclamation.

1. INTRODUCTION

Semi-enclosed bays have been suffering from eutrophication and oxygen-deficit in bottom water in many countries[1)]. Eutrophication is the excessive enrichment of aquatic ecosystem, which leads to increase in primary production, noxious algal bloom, food chain alteration and depletion of dissolved oxygen, and is a continuing and growing problem in many part of the world. While hypoxic and anoxic environments have existed through geological time, their occurrence in shallow coastal and estuarine waters appears to be increasing, most likely accelerated by human activities[2)]. Eutrophication acts as an enhancing factor to hypoxia and anoxia and when coupled with adverse meteorological and hydrodynamic events, these increase in frequency and severity[2)]. Hypoxia and anoxia have a critical impact on the living resources and may cause a serious damage to fishery[3)]. The spatial and temporal distribution and severity of hypoxia and anoxia in a coastal ecosystem vary from year to year and are related to a combination of factors, including meteorology and freshwater runoff, both of which directly affect the magnitude of primary production and stratification of the water column[4)]. Increased primary production results an increased organic loading, which is oxidized in the water column or bottom sediment. In stratified water, decomposition of organic material in the bottom water, which has limited oxygen supply due to stratification result in hypoxic conditions[5)] and are usually occur during the warmer months. Under low oxygen conditions, the sulfide compounds in the bottom sediments increased, which can cause serious damage to the benthic fauna[6)]. Under some wind conditions upwelling of this oxygen-depleted water would occur, causing surface water having low dissolved oxygen, occurrence of blue tides and death of fishes. Land reclamation in coastal areas is very common in Japan. This may lead to the development of dead water zones, thus changing the current and mixing of water and also has significant impact on water quality and the formation of oxygen-deficit water. However, very few works have been conducted to quantify the environmental impact of land reclamation works on water quality, especially of the formation of oxygen deficit water.

Hakata Bay, a semi-closed bay located in the western part of Japan, has been a topic of intensive research for the last few years because of eutrophication and occurrence of algal blooms and red tides at water surface and the onset of hypoxic and anoxic conditions at bottom waters in every summer caused by large quantities of pollutant loads from Fukuoka City and its catchments. The longitudinal and latitudinal lengths of the bay are about 20 km and 10 km, respectively. The watershed area is about 690 km^2 and a population of about 1.9 million lives in this area. The bay has an average water depth of 10 m below the mean sea level. The average air temperature is as high as 28^0C in August and as low as 7^0C in January. The depth-averaged salinity lies in a narrow range of 29-34 ppt. Moreover, high growth of phytoplankton and associated high primary production during the winter is observed in spite of low water temperature, which is characterized a special phenomenon affecting water quality of the bay[7]. Land reclamation of about 401 ha areas is also going on in the inner bay (**Fig.1**), which will be completed by the year 2004.

This study was concentrated mainly to the eastern (inner) part of the Hakata Bay (**Fig.1**), which is the most affected area of the bay due to eutrophication. The occurrence of hypoxia and anoxia in this area may be developed under specific combination of flow, density stratification and material circulations in the system. Therefore, a 3-D time-dependent combined hydrodynamic and eutrophication model (CHEM) was developed to simulate the processes controlling the formation of oxygen-depleted waters in the bay. Atmospheric heat fluxes through the water-surface that governed the thermal structure of shallow waters were explicitly considered in the model by incorporating a heat transfer sub-module. A fully predictive benthic-sediment diagenesis process was also incorporated in the model. The model was calibrated with the observed data in 1996-97.

In this paper, we first briefly describe the salient feature of the combined hydrodynamic and eutrophication model. Although the tolerance of aquatic life to hypoxia is well known, evaluation of the probable damage and severity caused by hypoxia on an ecosystem remains difficult, however it depends on the occurrence probability of these events. Since the physical and biological processes occurring within a water environment are inherently random[8], probabilistic calculations of the occurrence of hypoxia and anoxia are more realistic and informative which represent also an indirect measure of the probable spatial and temporal damage and severity caused by hypoxia and anoxia on the living resources in the ecosystem. If the occurrence

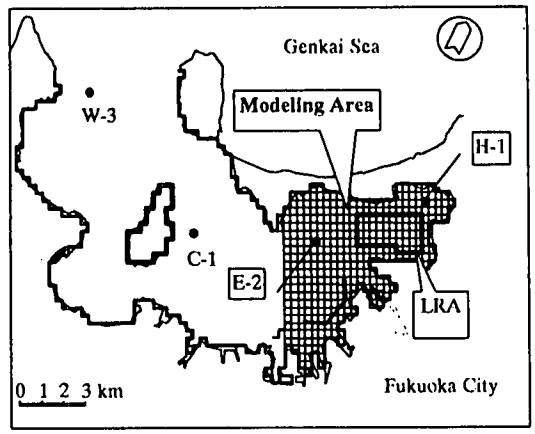

LRA – Land Reclamation Area • Monitoring Stations

Fig.1 Hakata bay, modeling area, water quality monitoring stations and model grid.

probability of hypoxia and anoxia in a particular time interval is high, its subsequent adverse effects and severity will also be high. This paper presents a methodology of calculating the probability of occurrence of hypoxic and anoxic waters and was applied to the study domain to assess the impact of eutrophication on the living resources. Meteorology has a significant influence on the formation of oxygen-deficit waters, so long-term simulations with observed meteorological data for 20 years (1980 to 1999) were carried out to investigate the interactions of meteorology and the formation of hypoxic and anoxic waters and the succeeding probability of occurrence and duration of these events. Moreover, an assessment of the ongoing land reclamation work on the formation of oxygen-deficit waters was also investigated using the model.

2. MODEL DESCRIPTION

(1) Hydrodynamic model

As part of the effort to simulate hydrodynamics and thermal behavior of the bay, a multilevel stratified flow model MK2[9] was used. MK2 is based upon the finite difference numerical solution of a set of 3-dimensional equations of motion and momentum, assuming hydrostatic pressure. The model calculates the tidal currents, diffusion between layers, water surface elevation, salinity and water temperature considering density flow and wind-induced current. The thermal stratification of shallow surface waters is mostly governed by atmospheric heat fluxes through the water surface and its distribution within the water body. The accuracy and potential success of any ecological model depend upon accurate simulation of water temperature, since the rate of chemical reactions as

well as biological activities in an aquatic system is mediated by water temperature. Fish survival and growth potential are significantly influenced by water temperature. Transport and mixing, therefore, recycling of key water quality parameters such as nutrients and dissolved oxygen are also significantly influenced by the stratification regime[10),11)]. The existing version of MK2, however, is not capable of treating atmospheric heat flux through the water body, so a heat transfer sub-module for the atmospheric radiation and sensible and latent heat fluxes was developed to simulate the hourly solar radiation input and its distribution within the water body. **Fig.2** shows the schematic diagram of these processes. The net rate of heat exchange per unit area of air-water interface can be written as:

$$H_n = (H_{sn} + H_{an}) \pm H_C - H_e - H_b \qquad (1)$$

in which, H_n= the net heat input at the water surface, H_{sn} = the net short wave solar radiation, H_{an} = the net atmospheric long wave radiation, H_C = the conductive loss, H_e = the evaporative loss (latent heat) and H_b = the back radiation. The components of heat budget **(Eq.1)** were computed by exact or semi-empirical equations in literatures[12),13),14)] using the observed daily meteorological variables (cloud cover, wind speed, atmospheric pressure, relative humidity, air and water temperature). The long wave portion of solar radiation is absorbed at the water surface and three principles[15)] were considered in calculating the net heat absorbed by a water surface (i=1) and attenuation of solar radiation with depths (i=2,m): (i) Net long wave atmospheric radiation, H_{an} is absorbed completely at the water surface, (ii) net short wave solar radiation H_{sn} is absorbed exponentially with depth based on water attenuation coefficient and (iii) losses or gains at the water surface caused by conduction H_C, evaporation H_e and back radiation H_b and can be utilized to determine solar attenuation with depth by the deep layers. The Beer-Lambert Law is used to determine solar attenuation with depth as follows:

$$H_{sn}(i) = \eta\, \Delta z . H_{sn}(i-1) \exp(-\eta . Z) \qquad (2)$$

in which, $H_{sn}(i)$ = attenuation of net solar radiation for the i^{th} horizontal layer, η = water attenuation coefficient (m^{-1}), Δz = thickness of the i^{th} water layer (m) and Z = depth of i^{th} water layer from surface (m). Depending on the relative significance of radiation input and losses, three cases described by Stefan and Ford[15)] was considered in each time step. The climate data (atmospheric pressure, cloud cover, air temperature, etc) provided by the Fukuoka Meteorological Observation was used to calculate

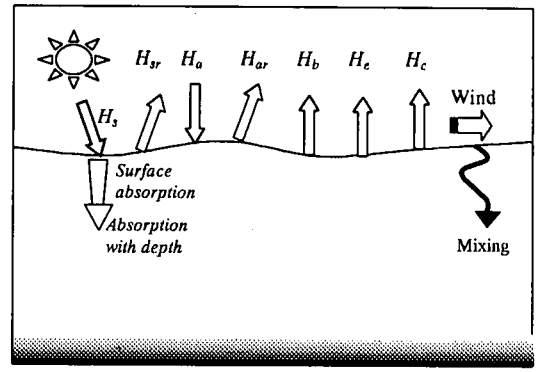

Legend:
H_s - Solar Radiation; H_{sr} - Reflected Solar Radiation
H_a - Atmospheric Radiation; H_{ar} - Reflected Atm. Radiation
H_b - Back Radiation; H_e - Evaporative Heatflux
H_c - Conductive Heatflux

Fig.2 Schematic diagram of heat budget showing heat flux components.

net hourly input of solar radiation. At the open boundary, the M_2 tidal constituent was specified with an amplitude of 54.4 cm by a phase lag of 192.2 degree. Moreover, hourly wind data (speed and direction) was inputted in the model to calculate wind-induced circulations. The initial conditions of water temperature and salinity at each layer are also specified and velocity at each layer is set to zero. The average freshwater inflows from tributaries and land areas (wastewater treatment plants, industries, etc) to the study area are about 15.43 m^3/sec and are specified daily based on the observed data[16)].

(2) Eutrophication model

The eutrophication model is an integrated model of material circulation between water column and bottom sediment, which incorporated nine state variables such as organic and inorganic phosphorus, organic, ammonia and nitrates nitrogen, COD and DO and two biological components, phytoplankton and zooplankton as shown in **Fig.3**. These state variables are considered as five interacting systems: dissolved oxygen balance, nitrogen and phosphorus cycle, phytoplankton and zooplankton kinetics. The structure of the model is based on a generally accepted framework[17),18),19),20),21),22),23)] with the exception of the interaction between the layers via vertical advection and turbulent diffusion. It solves the partial differential equations describing the conservation of mass and momentum of the incompressible fluid pollutants over the depth of each layer for a multi-layer representation.

The eutrophication model is a modification and extension of our previous model[23)] into multi-layer representation for coastal bays. In the model, two types of phytoplankton, one grows at higher temperature and other at lower temperature (winter) was

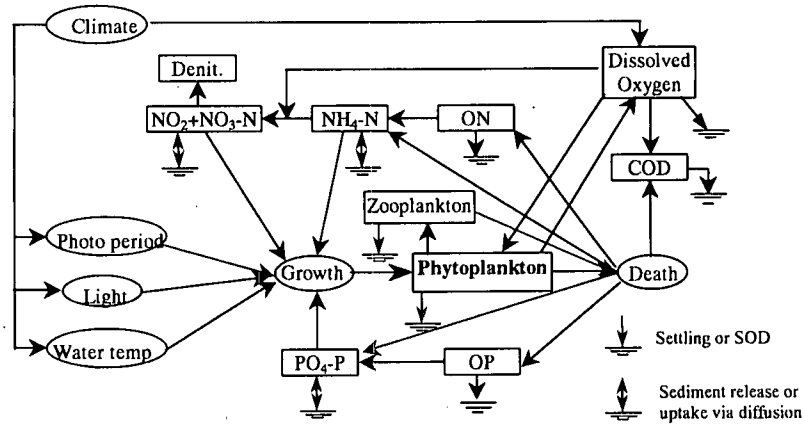

Fig.3 Schematic diagram of kinetic interactions in the water column.

considered. Due attention was paid to simulate zooplankton dynamics, because zooplankton provides a dynamic closure to the predation term in phytoplankton production equation. The growth rate of algae depends on three principal components; temperature, solar radiation and nutrients[18),19),24)]. The temperature dependence for the algal growth at higher temperature *g(T1)* and that at lower temperature *g(T2)* are expressed as:

$$g(T1) = 2.30\exp[0.085(T-18)] \tag{3}$$

$$g(T2) = 0.35\left[\frac{T}{10}\exp(1-\frac{T}{10})\right]^{2.5} \tag{4}$$

where, T is the water temperature in ^{o}C. The light limitation function of Steel and Baird[18)] is used for both group of phytoplankton. All the individual nutrients (N, P) are computed by Michaelis-Menten type expression and the lower value is chosen for nutrient limiting factor.

Hydrolysis and bacterial decomposition of organic nitrogen and phosphorus depend on water temperature and phytoplankton biomass and saturating recycle expressions based on algal biomass is used to describe this dependency. The kinetics of complete nitrification is modeled as a function of ammonium, DO and temperature, based on the concept proposed by Tuffey *et al.* 1974[20)] as:

$$NT = \frac{DO}{K_{NT}+DO}\cdot\frac{NH_4}{K_{NH4}+NH_4}f(T) \tag{5}$$

where, K_{NT} = the half-saturation constant of DO required for nitrification (mg/L) and K_{NH4} = the half-saturation constant of NH_4-N required for nitrification (mg/L). The denitrification process is modeled by the first order transformation, which depends on DO, temperature and nitrite plus nitrate nitrogen concentration as:

$$DT = \frac{K_{DO}}{K_{DO}+DO}\cdot\frac{NO_2+NO_3}{K_{NO3}+NO_2+NO_3}f(T) \tag{6}$$

where, K_{DO} = the half-saturation concentration of DO required for oxic respiration (mg/L) and K_{NO3} = the half-saturation concentration of nitrate required for denitrification (mg/L). The deoxygenation (k_c) of COD is considered to depend on water temperature and dissolved oxygen concentration as:

$$k_c = \frac{DO}{K_{COD}+DO}f(T) \tag{7}$$

where, K_{COD} = the half-saturation concentration of DO required for exertion of chemical oxygen demand (mg/L). Saturation concentration of DO in water depends on both water temperature and salinity and the equation developed by Hyter *et al.*[17)] is used in the model to calculate DO saturation.

(3) Sediment-water interactions model

Exchange of material between the water column and benthic sediments is an important component of the eutrophication process. The sediment model consists of three basic processes: deposition of particulate organic carbon, nitrogen and phosphorus (POM) including dead and respired phytoplankton and zooplankton from the water column to the bottom sediment; decay or diagenesis of POM within the sediment layers to produce inorganic substances (NH_4-N, NO_3-N and PO_4-P) and release or flux of these substances to the water column and to the deep inactive sediment layer via diffusion. Nutrients undergo adsorption and desorption or precipitation and dissolving between the interstitial liquid phase and solid phase in mud. The release of phosphate from sediment is markedly controlled by the oxidation-reduction potential (ORP) condition.

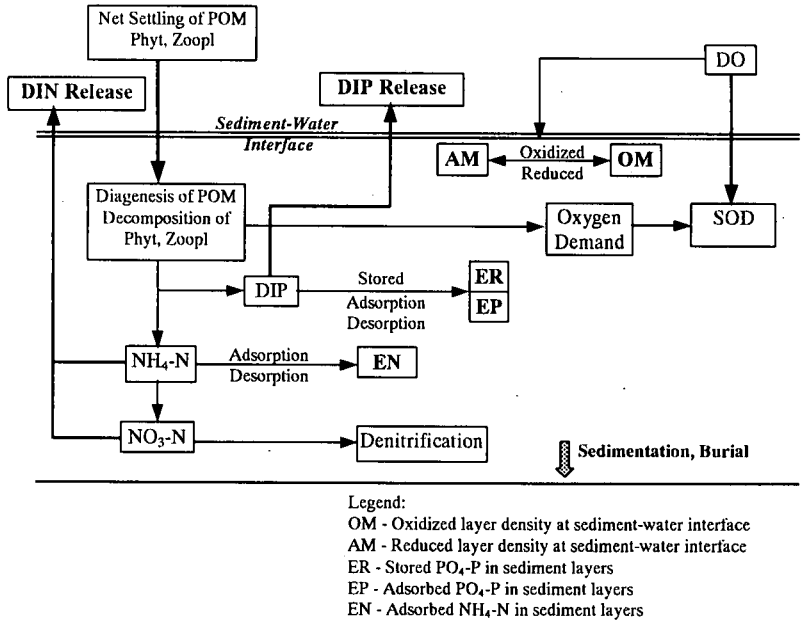

Fig.4 Schematic representation of the diagenetic sediment model.

If the DO condition above the bottom sediment is high, an oxidized layer (ferric oxide) is formed by the reaction of DO above the sediment and ferrous iron in the upper layer of the mud, which can adsorb certain amount of PO_4-P formed by the degradation of organic substances. Mass flux through the sediment-water interface is dominated by bioturbulation under aerobic condition[25]. If DO is deficient, sulfide is formed, reducing oxidized layer and the adsorbed PO_4-P are released equivalently[26]. The schematic diagram of the benthic sediment diagenesis process is shown in **Fig.4** and the mathematical formulations of the anaerobic break-down and decomposition of POM, detritus algal and zooplankton are taken from the works of Nakanishi *et al.* 1986[26]. Anaerobic breakdown and decomposition of organic detritus are sinks of the oxygen and rapidly derive its concentration negative, indication that the sediment is reduced rather than oxidized[27]. The fluxes of oxygen (SOD), DIN and DIP across the sediment-water interface are computed from the respective water column and benthic layer concentrations using Fickian diffusion approach.

(4) Model schematization

The layer-averaged water quality variables and transport equations of pollutants solved in the model are defined and derived in a similar way to those of MK2. The water quality algorithms are integrated directly into the hydrodynamic model, so that they share the same computational grid and time steps and run simultaneously. Computational domain was divided into staggered meshes in the Cartesian coordinates with the horizontal grid of 300m x 300m (**Fig.1**). The model uses a z-coordinate system that discretizes the water depth into 5 layers with variable thickness. The top water layer is 1m thick, while the second, third and forth layers are 3m, 3m and 4m, respectively. The rest is thickness of the last layer. The number of layers at each grid depends on water depth and the thickness of top layer varies with water level fluctuations. The sediment layer is divided into two layers, the top one is 1cm and the bottom layer is 5 cm thick. Free surface elevation and layer-averaged currents were calculated with the finite difference schemes of forward difference in time, upwind difference for the advection and the central difference for the diffusion term. The concentrations of all water quality variables at the open boundary are specified daily and the wastewater loadings from tributaries, treatment plants and industries were specified daily based on observation. To remove the effect of appropriate initial conditions, the model was run for one year and the last day values of all water quality parameters at each layer are assigned as the initial conditions.

3. MODEL CALIBRATION

(1) Hydrodynamic model results

Both the hydrodynamic and the eutrophication model was calibrated with the observed data for the whole period of the year from April 96 to March 97 to capture the entire range of the physical processes

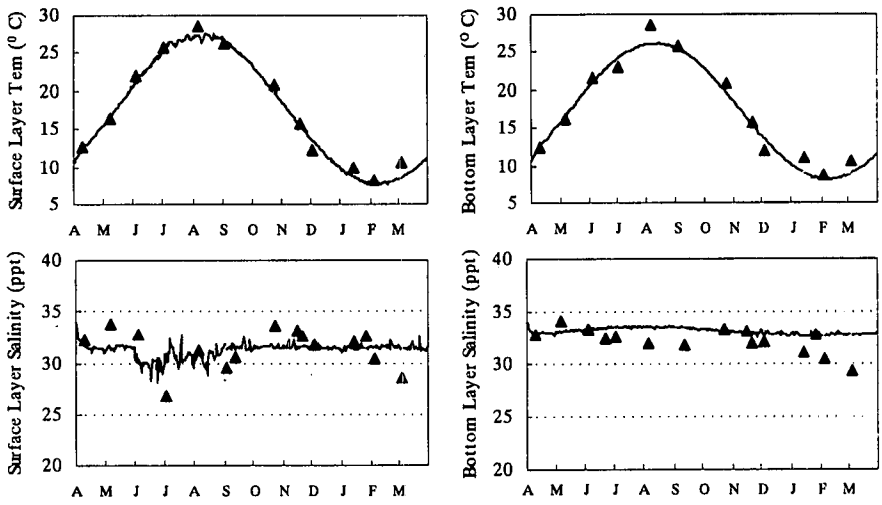

Fig.5 Layer averaged time series comparisons of water temperature and salinity at E-2 (5,9) during 1996-97.

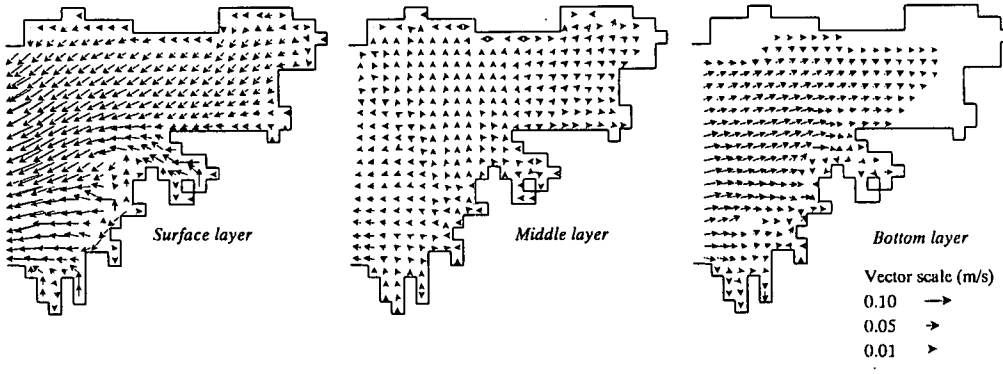

Fig.6 Flow patterns of the residual current in the inner Hakata bay during summer.

of the bay (well mixed conditions, vertical stratified summer period). The parameters used in the hydrodynamic model are presented in **Table 1**. Moreover, to test the effect of boundary condition on water circulations in the study domain, we simulated separately the hydrodynamics of the whole bay as well as for the study domain and compared the results of velocity ellipses at several stations in the study area as obtained from these two simulations. The velocity ellipses are almost similar; therefore, considering the open water boundary for the study domain is sufficient enough for this integrated modeling study. The simulated tidal ellipse of the M_2 constituent showed good agreement with the observation, however, the results are not showed here. The measured data shows that a temperature difference of about 0.3°C between the upper and lower layers existed in most of the period of a year except June and July, when a thermal difference of more than 1°C was observed. Salinity difference of about 6 ppt is observed between the surface and bottom waters in the rainy season, but for the other periods, the difference is insignificant. Model computed surface and bottom water temperature and salinity as compared with the observed data from those respective depths are illustrated in **Fig.5**. This result showed that the model could capture and reproduce the temporal change in water temperature of the bay accurately. However, some discrepancy is observed in salinity calculation, but the overall agreement between the simulated and observed salinity are good. The computational results of the residual currents, which are obtained by integrating simulated currents over one tidal cycle, are shown in **Fig.6**. An outflow circulation at the upper layer and an inflow circulation are dominated at the bottom. Therefore, a significant amount of the organic materials (externally inputted as well as that produced by primary production) is transported by the bottom residual current to the inner bay, where they accumulate and finally decompose and has a significant role in the material circulation and eutrophication process in bay.

Table 1 Parameters used in the hydrodynamic model.

Parameter	Value	Unit
Time step	10	sec
Coriolis' parameter	$8.1x10^{-5}$	1/sec
Roughness coefficient at the water surface and between the layers	0.001	
Roughness coefficient at the bottom	0.0026	
Horizontal diffusion coefficient of temperature and chlorinity	5.0	m^2/sec
Specific heat	3930.0	J/kg/^{0}C
Latitude of the basin	33.67	Degree
Longitude of the basin	130.33	Degree
Elevation of the basin	0	m
Evaporation coefficient (AE)	0.00068	ft/hr-in of Hg
Evaporation coefficient (BE)	0.00027	ft/hr-in of Hg.mph
Dust attenuation co-efficient	0.12	

(2) Eutrophication model results

The yearlong computed water quality parameters as compared with the observed data for Chl-a, DO, organic phosphorus, PO_4-P, organic nitrogen, NH_4-N and NO_2+NO_3-N from April 96 to March 97 are shown in **Fig.7** and the resulting kinetic parameters and the coefficients are shown in **Table 2.** Some of the parameters are specified based on observation. The oscillation in model predictions for Chl-a and other variables reflects the complexity of the ecological processes. It may be caused by several reasons, including the considerable variation of light intensity, pollutant loadings, tidal flow, density stratification, water temperature, wind speed, salinity, etc. As shown in **Fig.7**, the computational results by the multi-layered 3D model mimic the measured data, i.e., the model could represent reasonably the algal growth dynamics and water quality processes in each layer of the Hakata Bay. However, some discrepancy is observed in some water quality parameters like PO_4-P in summer time. This happens mainly due to the growth of other dominant species like *Aosa*, which was not considered in the model due to lack of data. In summer, significant amount of *Aosa* is grown in Hakata bay by taking inorganic phosphorus for growth and may cause this disagreement. The seasonal variation of Chl-a and COD at the surface layer is well predicted and have the same tendency, suggests that organic pollution of the bay is closely associated with the primary production. The computational results showed reasonably the stratification tendency in all other water quality variables, which is consistent with the density stratification of the bay. Hakata Bay waters in summer are weakly mixed due to the combined effects of freshwater inflows and meteorology, which result an obvious multi-layered feature. Serious oxygen depletion and anoxic and hypoxic conditions may appear in the bottom layer, while the surface water may still be well oxygenated. The computed DO, especially for the bottom water is

Table 2 Kinetics and stoichiometric parameters used in the eutrophication and sediment model.

Parame-ter	Description and unit	Value
K_{mNN}	Half-saturation constant for nitrogen uptake, μg N/L	15.0
K_{mNP}	Half-saturation constant for phosphorus uptake, μg N/L	1.50
K_{mpc}	Half-saturation constant for algae effect on mineralization, μg Chl-a/L	5.00
K_{NIT}	Half-saturation DO constant for oxygen limitation of nitrification, mg O_2/L	1.00
K_{DN}	Half-saturation DO constant for oxygen limitation of denitrification, mg O_2/L	0.50
K_{COD}	Half-saturation DO constant for CBOD deoxygenation, mg O_2/L	0.50
K_{NH4}	Half-saturation constant of NH_4-N required for nitrification, mg N/L	1.00
K_{NO3}	Half-saturation constant of NO_2+NO_3-N required for denitrification, mg N/L	0.10
C_g	Grazing (filtering) rate of zooplankton, L/ mg ZooplC/day)	0.30
K_Z	Half-maximum efficiency food level for zooplankton filtering, μg Chl-a/L	5.00
I_S	Saturated light intensity of algal growth, ly/day	150.0
k_{OP}	Mineralization rate of OP to PO_4-P, day^{-1}	0.002
k_{ON}	Mineralization rate of ON to NH_4-N, day^{-1}	0.008
k_d	Decay rate of COD, day^{-1}	0.10
k_{CN}	Nitrification rate of NH_4-N to NO_2+NO_3-N, day^{-1}	0.40
k_{CNN}	Denitrification rate, day^{-1}	0.055
f_{OP}	Fraction of dead and respired algae and zooplankton recycled to OP pool	1.0
f_{ON}	Fraction of dead and respired algae and zooplankton recycled to ON pool	1.0
f_{DOP}	Fraction of dissolved organic phosphorus in the totals	0.40
f_{DON}	Fraction of dissolved organic nitrogen in the totals	0.80
f_{PD}	Phosphorus/dry weight ratio of detritus	0.00757
f_{ND}	Nitrogen /dry weight ratio of detritus	0.0547
K_{PO4}	Partitioning coefficient of PO4-P, m^3/gm	0.20
CCHL	Carbon to Chl-a ratio	100.0
η	Zooplankton assimilated efficiency (mg ZooplC assimilated/mg ZooplC ingested)	0.50
a_{PC}	Stoichiometric ratio of cell phosphorus to algal carbon, mg P/mg C	0.012234
a_{NC}	Stoichiometric ratio of cell nitrogen to algal carbon, mg P/mg C	0.16765
a_{OC}	Oxygen to carbon ratio	2.67
W_S	Settling rate of phytoplankton, cm/day	20.0
W_D	Settling rate of detritus, cm/day	30.0
W_Z	Settling rate of Zooplankton, cm/day	0.0
W_{S4}	Settling rate of PO4-P sorbed, cm/day	40.0
W_P	Settling rate of particulate organic phosphorus, cm/day	20.0
W_N	Settling rate of particulate organic nitrogen, cm/day	40.0
γ	Porosity of sediment	0.78
ω	Volume/ weight ratio of pore water/ dry mud, mL/gm	1.3636
α	Adsorption equilibrium constant, gm/mL	0.25
β	Activity of oxidized layer for P-storing	0.30
K_{EP}	Adsorption/desorption rate coefficient of P, day^{-1}	0.0
K_R	Precipitation or dissolving rate coefficient of P, day^{-1}	0.864
K_{EN}	Adsorption/desorption rate coefficient of NH_4-N, day^{-1}	8.64
R_{dm}	Revision factor of diffusion coefficient for DO to that of PO_4-P	3.0
K_{MD}	Diminishing rate of oxidizing layer, day-1	0.03
K_{MP}	Production rate of oxidizing layer, day-1	0.03
W_M	Sedimentation rate of sediment layers, cm/day	0.01

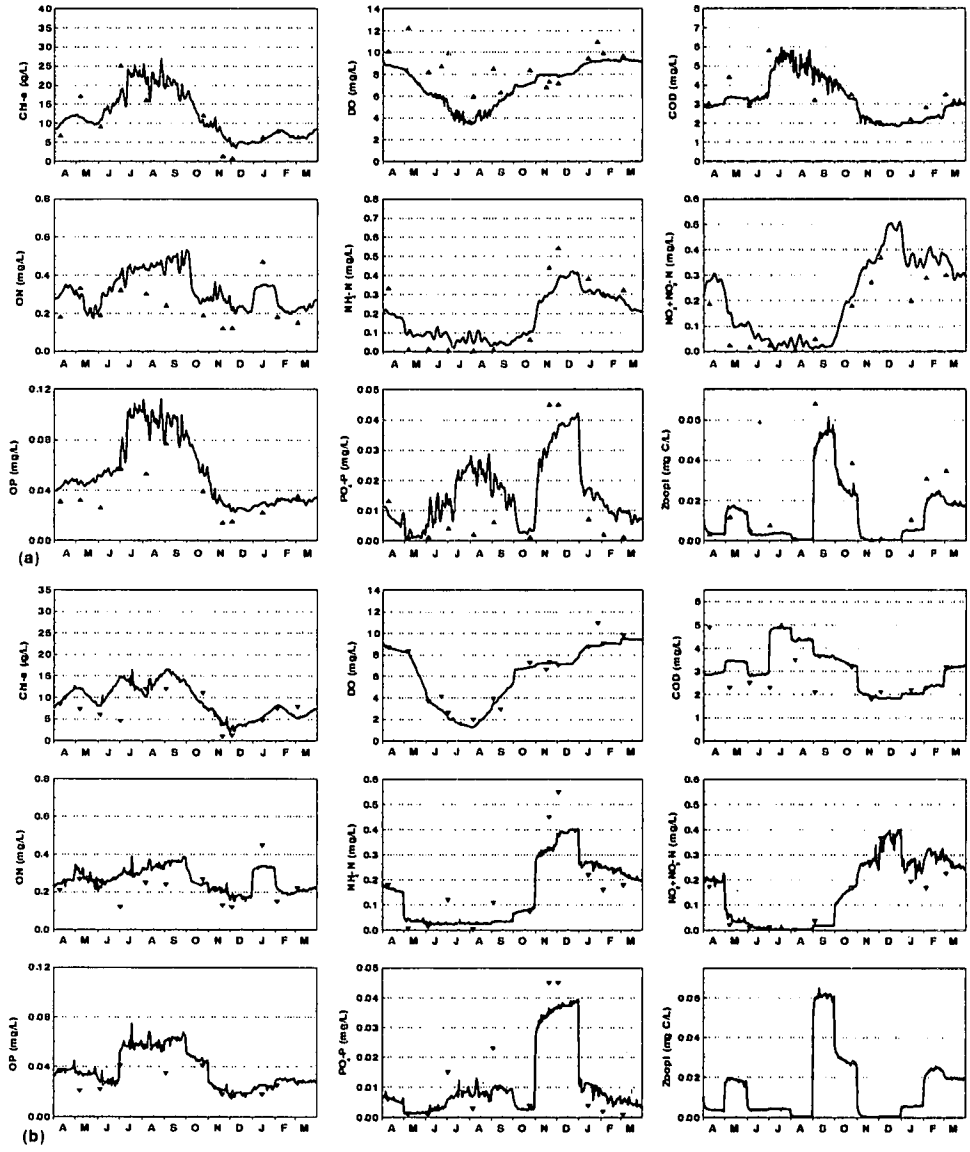

Fig.7 Layer averaged time series comparisons of results computed and measured at E-2 (5,9) during 1996-97: (a) surface layer and (b) bottom layer.

well agreed with the observation. During winter, water are well mixed and stratification almost diminishes and as a result, vertically uniform concentration of water quality may be attained. The model could reproduce this phenomenon reasonably well, thereby substantial its capability to capture the system behavior. The simulation also shows that zooplankton is an important factor affecting algal population in the bay and should be considered in the top-down control of algal population in the bay.

(3) Sediment-water interactions model results

The model calculation of sediment fluxes of DIP, DIN and SOD are shown in **Fig.8** and the kinetic and stoichiometric parameters of the sediment-water interaction model are presented in **Table 2**. Bottom water anoxia in summer, induces higher release of DIP and DIN from sediment. Temperature enhanced diagenesis and reduction of sorption capacity in surficial sediments due to lowering DO in bottom water produce maxima in DIP release. A time lag of about 2 months is observed between the maxima of DIP and DIN released. The optimal temperature for nitrification is less than peak temperature[20] and may cause this time lag in maximum release of DIN. Sediment oxygen demand is very high during summer and bottom oxygen-depletion is associated with higher SOD in summer. In general, SOD has a direct relationship with the productivity in the water column; it depends mainly on water temperature and

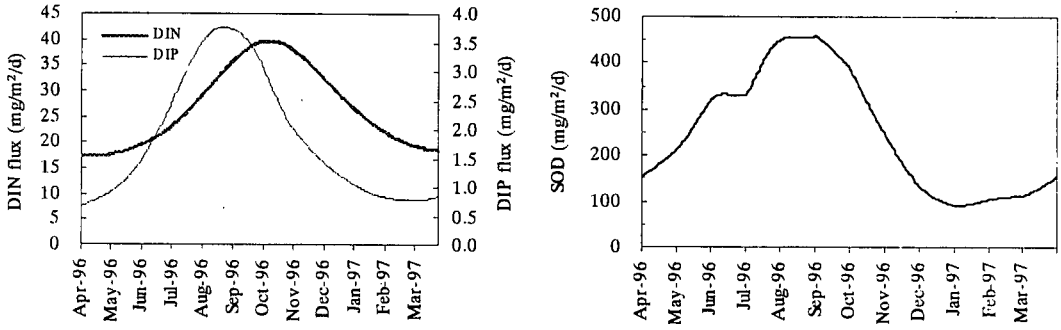

Fig.8 Model calculation of the seasonal fluxes of (a) nutrients and (b) sediment oxygen demand (SOD) at E-2.

amount of settle algal detritus. Model predicts also a significant amount of inorganic nutrients regenerated from the sediment throughout the year. In the model, nutrients released from the bottom sediment are modeled independent of water temperature, but as an interactive process between water column and bottom sediment.

4. PROBABILITY OF OCCURRENCE OF HYPOXIC AND ANOXIC WATER

Using the model, the probability of occurrence of hypoxic and anoxic conditions, duration of these events and wind condition that caused upwelling of bottom water having low DO in the inner Hakata bay were examined under observed meteorological conditions for twenty years period (1980 to 1999). There have been several definitions of the oxygen-deficit water depending on the degree of harmfulness to marine organism. The number of species and abundance of benthic organisms and fishes are strongly associated with the DO concentration in the near bottom water[28]. From the point of fisheries production and preference, the number of fish species and their diversity decreases drastically, when DO falls below 3.0 mL/L (1 mL/L = 1.45 mg/L) and almost all species of fish are influenced under DO less than 2.0 mL/L[29]. When DO drops to less than 3.6 mg/L, the normal distribution of benthos begins to change and mortality of yellowtail tuna[30] is initiated. Benthic infaunal and shellfish mortality will be initiated when DO drops below 2.0 mg/L[2),30]. Most coastal populations can tolerate short exposure to low DO, but exposure to less than 2.0 mg/L in seawater for one to four days causes the mortality of most fish and biota, especially during summer, when metabolic rates are high. Water having DO in between 0.036 mg/L to 3.6 mg/L is termed as oxygen-deficient water mass and DO of 0.036 mg/L is the upper limit of anoxic water mass[30]. In this study, DO of less than 3.6 mg/L and

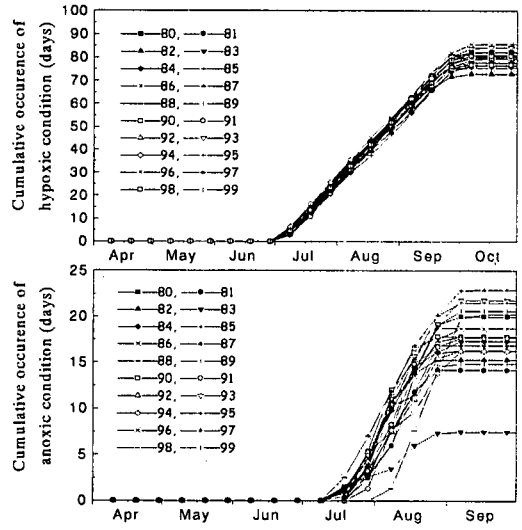

Fig.9 Cumulative occurrence of hypoxic and anoxic water at H-1 (22,3) for twenty years simulation.

0.036 mg/L were taken as the criterion for the hypoxic and anoxic water, respectively[30),31]. We define the probability of occurrence of hypoxia and anoxia that may occur in every 10 days in a certain layer of a grid location as:

$$P_{oh} = 100\frac{N_h}{N_T} \tag{8}$$

$$P_{oa} = 100\frac{N_a}{N_T} \tag{9}$$

in which, P_{oh} and P_{oa} = the occurrence probability of hypoxic and anoxic water, respectively, N_h and N_a = number of the occurrence of hypoxic and anoxic events in a time interval of 30 min within 10days and N_T = 10days/30 min = 480.

Fig.9 represents the cumulative occurrence of hypoxic and anoxic water at the head of the bay at station H-1 (22,3). Contours of the probability of occurrence and progressive development of hypoxia and anoxia in the bottom water are shown in **Fig.10**

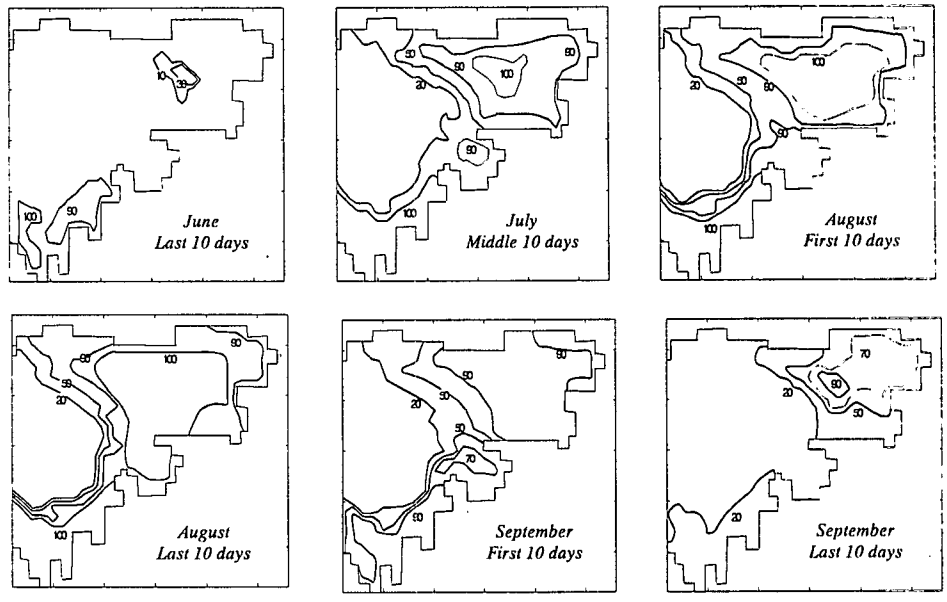

Fig.10 Contours of progressive development and probability of occurrence of hypoxic water (%) at the bottom of the inner bay averaged over 20 years' simulations from 1980-1999.

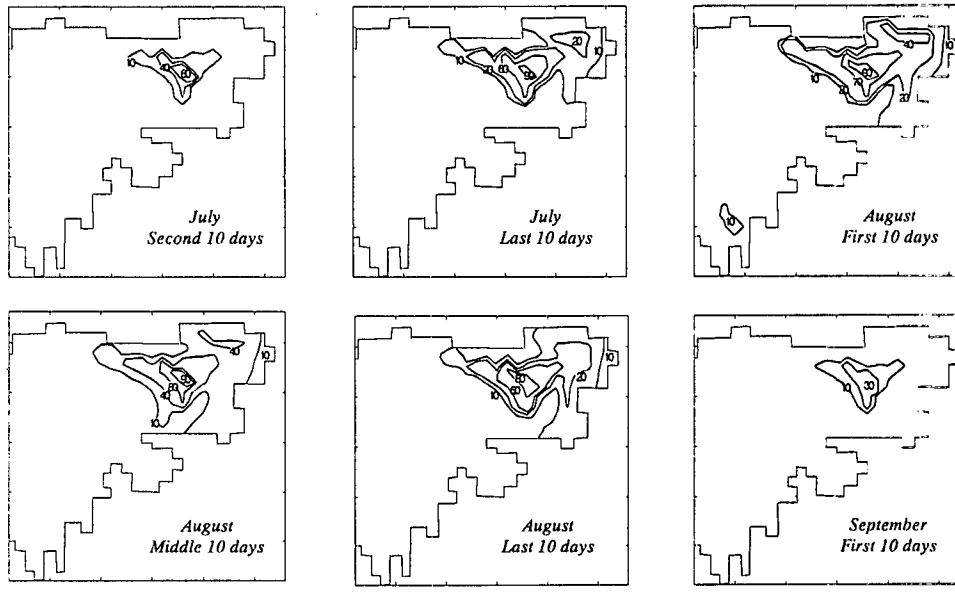

Fig.11 Contours of progressive development and probability of occurrence of anoxic water (%) at the bottom of the inner bay averaged over 20 years' simulations from 1980-1999.

and **Fig.11**. These contours are the averaged results of our simulations under a wide range of meteorological conditions for twenty years, thus represents the general trends and the most probable occurrence of hypoxic and anoxic conditions in a year. Seasonal hypoxia first appears at the end of June, and then gradually expanded and is most severe during August, when a larger portion of the bottom water is experienced by hypoxia having high probability of occurrence. The exposure to hypoxic water is also very high, so the potentially high damage and severity associated with hypoxia on the ecology are most intense in this period. Mortality of the most benthic organisms will occur and fish will die or disappear from this area due to prolonged hypoxia. By the end of September, hypoxia disappears by the onset of cooling and subsequent breakdown in the strength of water column stratification. Highest

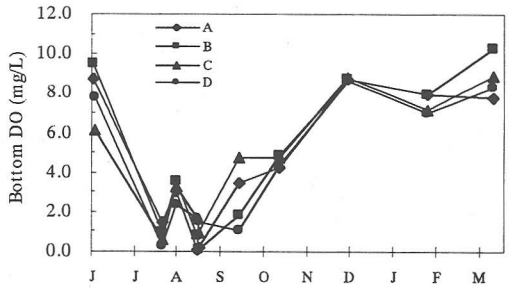

Fig.12 Bottom DO conditions from several stations in the inner bay in 1996-97.

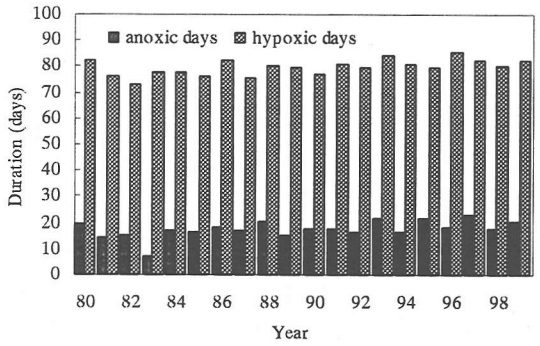

Fig.13 Model calculations of the duration of anoxic and hypoxic conditions in the inner bay.

water temperature is observed in August (**Fig.5**), which coincides with the highest probability of occurrence of hypoxia. Thus the stratification caused by climate condition is the major factor for the formation of oxygen-deficit water mass in the inner part of the bay. Anoxic water mass appears in the middle of July and disappears at the earlier days of September. However, between these periods, all days are not anoxic, rather it may occur intermittently, depending on stratification and meteorological conditions.

(1) Duration of hypoxia and anoxia

The bottom DO conditions of the inner bay from several measuring stations[32] during 1996-97 is shown in **Fig.12**. This survey results showed that oxygen-depleted water mass occurred at the bottom water and hypoxic condition lasted for about 90 days. Anoxic condition also occurred, however no information about the duration of anoxia is available from this monthly-based survey. Model computation of the duration of hypoxia and anoxia (in days) at the bottom layer at H-1 is shown in **Fig.13**. This figure indicates that under the observed meteorological conditions in the study area, the development of hypoxic water mass and duration of the hypoxic condition at the bottom waters of the bay is almost similar in each year. However, meteorology has a significant influence in the development of anoxic

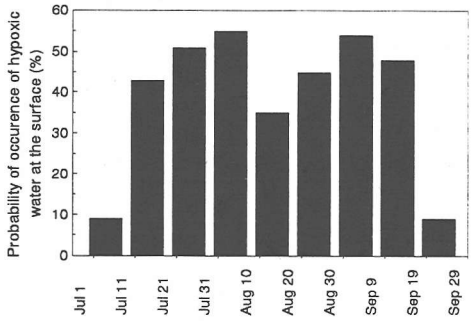

Fig.14 Occurrence probability of hypoxic condition at surface under meteorological condition in 1996.

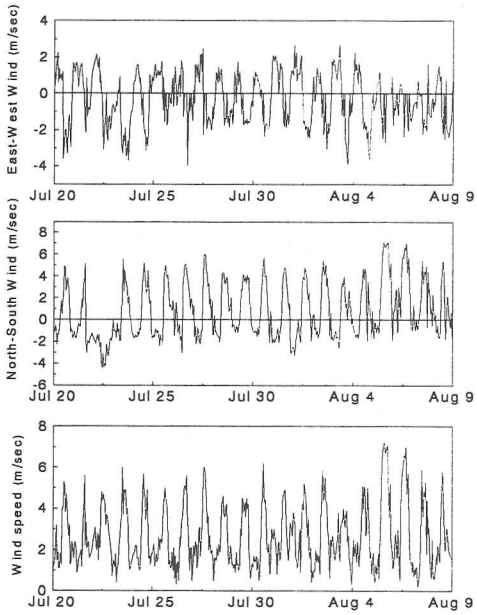

Fig. 15 Wind conditions that caused upwelling of bottom water during July 20 to August 8 in 1996.

bottom waters and the existence of anoxia at the head of the bay is lowest under the meteorology of the year in 1983.

(2) Occurrence of hypoxia at surface water and wind conditions

Under some wind events, strong upwelling may occur and if the oxygen-depleted waters were present at the bottom layer at that time, can be brought to the surface by upwelling. Model results show that upwelling occurred every year causing hypoxic condition to some extent at surface water. Model computation of the probability of occurrence of hypoxic water at surface layer in 1996 is shown in **Fig.14** and the wind conditions that caused upwelling and the maximum probability of occurence of hypoxia during July 20 to August 8 in 1996 are shown in **Fig.15**. In order to quantify the wind

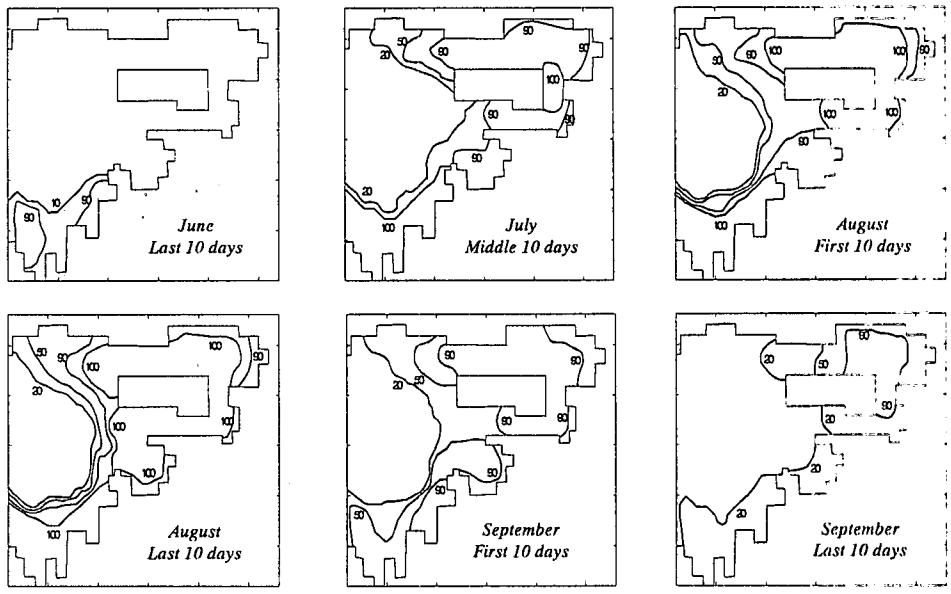

Fig.16 Contours of progressive development and probability of occurrence of hypoxic water (%) at the bottom of the inner bay with land reclamation work averaged over 20 years' simulations from 1980-1999.

condition that caused upwelling of bottom oxygen depleted water to the surface, multiple regression analysis of the probability of occurrence of hypoxic condition at surface and wind speed and direction during July 20 to August 8 for twenty years was conducted. A distinct wind patterns are observed in day and night time in the study side. Therefore, we divided the observed wind into two categories; daytime wind and nighttime wind and again divided each wind into westerly and southerly components. The multiple regression analysis gives the following correlation with a maximum error of 5.72%.

$$Y = 2.0773V_{WD} - 1.3213V_{SD} + 4.2396V_{WN} - 2.3889V_{SN} + 48.4816 \quad (10)$$

in which, Y = the probability of occurrence of hypoxic water at surface (%), V_{WD} and V_{WN} = the average westerly wind in day and night time respectively (m/sec) and V_{SD} and V_{SN} = the average southerly wind in day and night time respectively (m/sec). As the coefficients of V_{WD} and V_{SD} are lower than V_{WN} and V_{SN}, the above relationship indicates a lower probability of occurrence of hypoxic condition at surface water during daytime than that occurs during nighttime. In daytime, DO content at surface water is high and get saturated in the afternoon by photosynthesis activity and upwelling of bottom DO depleted waters are quickly mixed with surface water, results in the less possibility of occurrence of hypoxic condition at the surface water. Winds in the nighttime can cause the higher probability of occurrence of hypoxic condition at the surface, as the DO in the nighttime is less. This analysis also indicates that the northerly and northwesterly wind has positive correlation with the probability of occurrence of hypoxic condition at surface water at the head of the bay and upwelling of the bottom oxygen depleted water to the surface, which also confirmed the upwelling phenomena of the semi-enclosed bay[33]. However, the incidence of hypoxic condition at surface water is intermittent depending on wind conditions.

5. ASSESSMENT OF THE LAND RECLAMATION WORK (LRW)

We also investigated the influence of the ongoing land reclamation work on the water quality and the formation of oxygen depleted water in the inner bay. For the purpose, we run the model with land reclamation area (LRA) for twenty years and compared the results with our previous simulations. Model calculation of the progressive development and the probability of occurrence of hypoxic water with LRA averaged over 20 years' simulations are shown in **Fig.16**. As compared with **Fig.10**, it is observed that the land reclamation work has no significant impact on the formation of the oxygen-depleted bottom water. However, it shifted the highest oxygen-depleted water (area with low DO) toward the north edge of the artificial island, which agreed with the results of previous simulation[3]. The

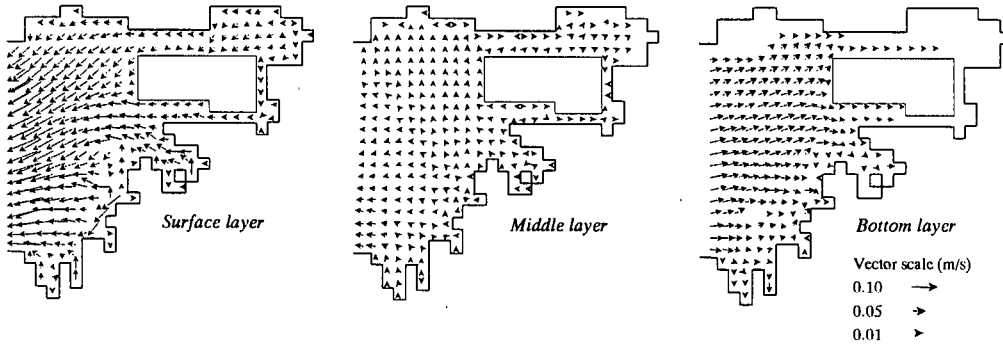

Fig.17 Flow patterns of the residual current in the inner Hakata bay during summer with LRA.

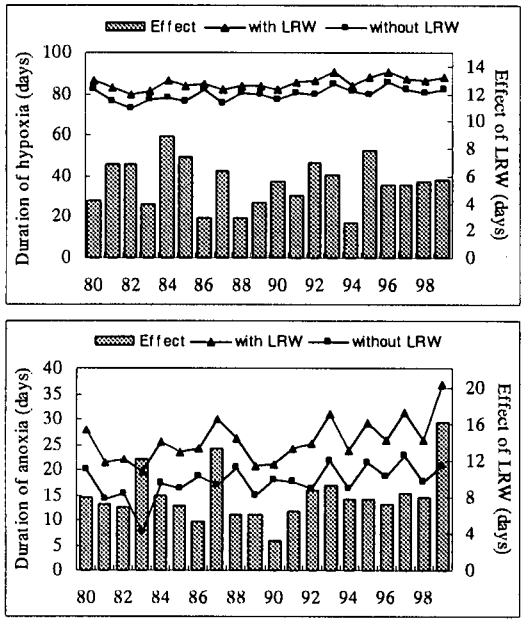

Fig.18 Effect of land reclamation work on the duration of hypoxic and anoxic conditions in the inner bay.

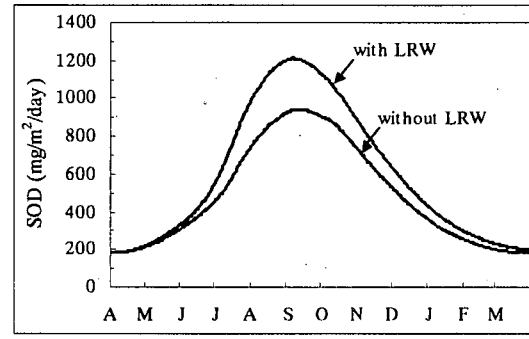

Fig.19 Effect of land reclamation work on sediment oxygen demand at H-2 (22,3).

simulated circulation patterns of the residual current with LRA are shown in **Fig.17**. The calculated durations of hypoxia and anoxia waters in the north edge of artificial island at (22,3) and the resulting effect of land reclamation work (LRW) are shown in **Fig.18**. The bar diagram represents the net increase of the duration of hypoxic and anoxic conditions. It shows clearly that the LRW prolongs the duration of hypoxic and anoxic conditions in the inner bay.

The algal growth rate as well as the primary production is not influenced and the circulation patterns of the residual current with artificial island are also similar to that without LRA (**Fig.6**). Thus, the same quantity of the organic matters as transported by the bottom residual current before (without LRA) to the inner bay, are accumulated to a narrower area at the north edge of the artificial island. As a result, the deposition rates increase in this area. Since the water temperature is not affected by artificial island, it will need a longer time to be decomposed. **Fig.19** shows that SOD at the head of the bay will be increased due to the construction of artificial island. The released rate of nutrients will also be increased. Thus, exert of higher SOD and lengthened in the decomposition time are seemed to be the main reasons of the prolonged duration of hypoxia and anoxia at the head of the bay due to artificial island.

6. SUMMARY AND CONCLUSIONS

Flow and pollutant transport in a natural water body is commonly interacted with density stratification and a multi-layered model is needed to describe the process reasonably. In order to simulate the oxygen-depleted water mass in the inner part of Hakata Bay, a multi-level integrated hydrodynamic and eutrophication model was developed. The integrated approach is a viable technique for understanding and predicting the water quality processes in the coastal bays. The comparison of yearlong calculation results with monitoring data in 1996-97 shows that the model could represent reasonably the algal growth dynamics and the importance features regulation biological and chemical processes of the

bay. Although some discrepancy is observed in some water quality constituents, the overall agreement between observation and simulation is reasonable and the model would follow the observed trend of the water quality constituents. The computed results also show that the present model could reasonably reproduce the stratification tendency of the water quality constituents in the bay.

During the summer, oxygen-depletion to hypoxic and anoxic conditions in the bottom waters occur as a result of increased stratification and enhanced decomposition of organic matter. Stratification first developed by excessive tributaries inflows in June and is progressively strengthening by the climate condition, i.e. with the increased in air temperature. In August, a larger part of the bottom water of the inner bay is experienced by hypoxia, when the water temperature is also highest. Another important factor affecting the formation of oxygen-depleted waters is the hydrodynamic condition that is the current patterns in the bay. The residual current towards the inshore dominates at the bottom waters, thus a significant amount of the inputted organic materials as well as that produced by algal blooms are transported by the bottom residual current to the inner bay, where they settled and decomposition and benthic respiration of these organic detritus add high SOD and also contributing to the development of hypoxic condition of the bay.

In this paper, we presented a statistical method of calculating the occurrence probability of hypoxia and anoxia to evaluate indirectly the probable spatial and temporal damage caused by these events on the living resources. The highest occurrence probability of hypoxic condition in a larger part of the bay is observed during August, which indicates that the severity of hypoxia including mortality of fishes and benthic community are also most intense in this period. During the survey period in 1996-97, the project area for land reclamation was surrounded by thick polyester curtain down to the bottom, thus the effect of land reclamation was existed during the survey. Hypoxia that occurred in the bottom water in the inner bay in 1996 was about 90 days and the model computed duration of hypoxia for the same year is about 91 days with land reclamation work (**Fig.18**). This indicates that the present model could capture the processes controlling the development of oxygen-depleted water in the bay very accurately. Hypoxic condition lasted for a prolonged time in the bay and under prolonged hypoxia, fish and invertebrates die and energy are dissipated by micro-benthos. Strong wind can cause the upwelling of bottom oxygen-depleted water and cause the development of hypoxic condition to some extent at the surface. Statistical analysis shows that upwelling of bottom oxygen-depleted water would occur at the head of the bay under the wind blowing towards the offshore either northerly or northwesterly. The ongoing land reclamation work has insignificant effect on the water quality, but it will shift the lowest DO area towards the north edge of the artificial island and will prolong the duration of hypoxic and anoxic conditions in the inner bay.

Though the model developed in this study is capable of reasonably simulating the hydrodynamics, thermal structure and water quality processes of the bay, which are the key elements in the formation and analysis of oxygen-depleted water mass, it still has some limitations and further improvements are needed. In the model empirical estimation was used to calculate the sediment layers temperature. In shallow water body, bottom bed get heating by solar radiation and water column bed heat exchange is important and need to incorporate in the model. Moreover, the field data of SOD and nutrients fluxes are very limited and verification of the sediment-water interactions model results is needed. The methodology presents here is seemed to be an effective and convenient way of examining the possible damage and adverse effect associated with the occurrence of oxygen-depleted water on the aquatic population in management strategies. The model can be used for other lakes and bays, where knowledge of temperature and density stratification is important for assessing the water quality.

REFERENCES

1) Mimura, M., Tsukada, M. and Suzuki, M.: Simulation of the behavior of oxygen-deficit water in Tokyo Bay by three-dimensional water quality model, *Proc. Coastal Eng. Conf.*, pp. 3575-3587, 1998.
2) Robert, J.D. and Rutger, R.: Marine benthic hypoxia: a review of its ecological effects and the behavior responses of benthic microfuna, *Oceanogr. and Marine Biology: an Annual Review*, 33, pp. 245-303, 1995.
3) Sekine, M., Karim, M.R., Ukita, M. and Hamada, E.: Study on the influence of hypoxia on fish in coastal construction area, *MEDCOAST 99-EMECS 99 Joint Conf., Land-Ocean Interaction: Managing Coastal Ecosystems*, Antalya, Turkey, pp. 695-705, 1999.
4) Officer, C.B., Biggs, R.B. Taft, J.L., Cronin, L.E., Tyler, M.A., and Boynton, W.R.: Chesapeake Bay anoxia: origin, development and significance, *Science*, 223, pp. 22-27, 1984.
5) Pihl, L., Baden, S.P. and Diaz, R.J.: Effects of periodic hypoxia on distribution of demersal fish and crustaceans, *Marine Biology*, 108, pp. 349-360, 1991.
6) Nakata, K. and Kuramoto, T.: A model of the formation of oxygen depleted waters in Tokyo Bay, *Proc. Adv. Mar. Tech. Conf.*, Vol. 5, pp. 107-132, 1992.
7) Nakashima, M., Lee, I.C. and Kusuda, T.: Characteristics of primary production in an eutrophicated bay, *MEDCOAST 99 - EMECS 99 Joint Conf., Land-Ocean Interaction: Managing Coastal Ecosystems*, Antalya, Turkey, pp. 195-206, 1999.

8) Tung, Y. and Hathhorn, W.E.: Assessment of probability distribution of dissolved oxygen, *J. Environ. Eng.*, ASCE, 114(6), pp. 1421-1435, 1988.
9) Fujihara, M., Akeda, S. and Takeuchi, T.: Development of multi-level density flow model and its application to the upwelling generated by artificial structures, *Technical Report,* National Research Institute of Fisheries Engineering, Aquacul. & Fish Port, 14, pp. 13-35, 1992, (Japanese with English abstract).
10) DiToro, D.M. and Connolly, J.P.: *Mathematical models of water quality in large lakes. II: Lake Erie*, USEPA, Washington D.C., 1980.
11) Wodka, M.C., Effler, S.W. and Driscoll, C,T.: Phosphorus deposition from the epilimnion of Onondaga Lake, *Limnol. Oceanorg.*, 30 (4), pp. 833-843, 1985.
12) Edinger, J.E., Brady, D.K. and Greyer, J.C.: Heat exchange and transport in the environment, *Rep. No. 14, Cooling Water Res. Project (RP-49)*, Electric Power Research Institute, Palo Alto, Calif., 1974.
13) Linford, C. B. and Thomas, O. B.: The Enhanced Stream Water Quality Models QUAL2E and QUAL2E-UNCAS: Documentation and User Manual, *Rep. No. EPA/600/3-87/007*, USEPA, Athens, Ga., 1987.
14) McCutcheon, S.C.: *Water Quality Modeling, Vol-I*, CRC Press Inc, Boca Raton, Florida, 1989.
15) Stefan, H. and Ford, D.E.: Temperature dynamics in dimictic lakes, *J. Hydr. Div.*, ASCE, 101(1), pp. 97-114, 1975.
16) Port and Harbor Bureau of Fukuoka City.: *Data report of observation at Hakata Bay in 1996-97,* 1997.
17) Bowie, G.L, Mills, W.B., Porcella, D.B., Campbell, C.L., Pagenkopf, J.R., Rupp, G.l., Johnson, K.M., Shan, P.W.H., Gherini, S.A. and Chambulin, C.E.: Rates, constants and kinetics formulations in surface water quality modeling, *Rep. No. EPA/600/3-85/040*, USEPA, Athens, Ga., 1985.
18) Thomann, R.V. and Mueller, J.A.: *Principles of Surface Water Quality Modeling and Control,* Harper and Row Publishers, New York, 1987.
19) Ambrose, R.B., Wool, T.A., Connolly, J.P. and Schanz, R.W.: WASP.4, A hydrodynamic and water quality model, *Rep. No. EPA/600/3-87/039*, USEPA, Athens, Ga., 1988.
20) Cerco, C.F. and Cole, T.: User's Guide to the CE-QUAL-ICM Three-Dimensional Eutrophication Model, *U.S. Army Corps of Eng.*, Washington D.C., 1995.
21) Chapra, S. C.: *Surface water quality modeling*, WCB /McGraw-Hill, New York, 1997.
22) Chau, K.W. and Jin, H.: Eutrophication model for a coastal bay in Hong Kong, *J. Environ. Eng.*, ASCE, 124(7), pp. 628-8637, 1998.
23) Karim, M.R., Badruzzaman, A.B.M., Sekine, M. and Ukita, M.: Assessment of nutrients and dissolved oxygen in a river system in Bangladesh using a water quality model, *J. Environ. Syst. and Eng.*, JSCE, 664/VII-17, pp. 97-107, 2000.
24) Lee, J.H.W., Wu, R.S.S., Cheung, Y.K. and Wang, P.P.S.: Forecasting of dissolved oxygen in marine fish culture zone, *J. Environ. Eng.*, ASCE, 117(6), pp. 816-833, 1991.
25) Lee, I.C.: Study on management of water quality and fisheries resource in eutrophicated coastal area, *Doctoral Thesis*, Dept. of Civil Eng., Yamaguchi University, 1997.
26) Nakanishi, H., Ukita, M. and Kawai, Y.: Study on the modeling of the behavior of phosphorus released from sediments, *Ecological Modeling*, 31, pp. 105-123, 1986.
27) Lung, W.S.: *Water Quality Modeling, Vol-III*, CRC Press Inc, Boca Raton, Florida, 1989.
28) Imabayashi, H.: Effects of oxygen-deficient water on the benthic communities, *Bull. Japan Soc. Sci. Fish*, 49(1), pp. 7-15, 1983 (Japanese with English abstract).
29) Nagai, T. and Ogawa, Y.: Fisheries Production, *Sustainable Development in the Seto Inland Sea, Japan, from the viewpoint of fisheries*, Terra Scientific Publishing Company, Tokyo, pp. 61-94, 1997.
30) Yanagi, T.: A summary of symposium of oxygen-deficient water mass, *Coastal Oceanogr.*, 26(2), pp. 14-145, 1989 (Japanese with English abstract).
31) Sekine, M., Lee, I.C., Narazaki, T., Ukita, M., Imai, T. and Nakanishi, H.: Handling of dissolved oxygen in the Seto Inland sea fisheries ecological model, *Proc. of Environ. Eng. Research*, Vol. 32, pp. 301-310, 1995 (Japanese with English abstract).
32) Watanabe, M., Sekine, M., Hamada, Y. and Ukita, M.: Monitoring of sea environment by using snapping shrimp, *J. Environ. Syst. and Eng.*, JSCE, 643/VII, pp. 49-60, 2000 (Japanese with English abstract).
33) Yoon, J.S., Nakatsuji, K. and Muraoka, K.: Study of upwelling phenomena of anoxic water 'A-oshio', *Proc. of Coastal Eng.*, pp. 3447-3461, 1994.

(Received February 19, 2001)

富栄養化および埋立による湾内の貧酸素および無酸素水塊の発現確率シミュレーション

Md. Rezaul KARIM・関根雅彦・樋口隆哉・浮田正夫

博多湾奥部における酸素欠乏水塊の形成に至る過程およびその後の貧酸素・無酸素水塊の発現確率について解析するために，流体力学と富栄養化の統合モデルを開発した．計算結果と観測データを通年比較した結果，モデルは湾内の水質および溶存酸素の変化における重要な特徴を表し得ることが示された．貧酸素・無酸素水塊は，淡水流入と気象条件に起因する成層の形成により夏季に湾奥底部で発生し，8 月に最も著しいことがわかった．また，現在進行中の埋立事業は，水質に対しては大きく影響しないが，貧酸素・無酸素の継続時間を長くすることが明らかになった．